

Scientific Article

# Functional image guided radiation therapy planning in volumetric modulated arc therapy for patients with malignant pleural mesothelioma

Yoshiko Doi MD<sup>a</sup>, Tomoki Kimura MD, PhD<sup>a,\*</sup>,  
Takeo Nakashima PhD<sup>b</sup>, Yuki Takeuchi MD<sup>a</sup>, Ippei Takahashi MD<sup>a</sup>,  
Ikuno Nishibuchi MD, PhD<sup>a</sup>, Yuji Murakami MD, PhD<sup>a</sup>,  
Yasushi Nagata MD, PhD<sup>a</sup>

<sup>a</sup> Department of Radiation Oncology, Hiroshima University Hospital, Hiroshima City, Japan

<sup>b</sup> Division of Radiation Oncology, Hiroshima University Hospital, Hiroshima City, Japan

Received 3 September 2016; received in revised form 18 January 2017; accepted 25 January 2017

## Abstract

**Purpose:** To investigate the incorporation of functional lung image-derived low-attenuation area (LAA) based on 4-dimensional computed tomography (4D-CT) in volumetric modulated arc therapy (VMAT) planning for patients with malignant pleural mesothelioma (MPM) after extrapleural pneumonectomy.

**Methods and materials:** Twelve patients with MPM after extrapleural pneumonectomy were included. The primarily affected side was the right in 6 patients and the left in 6 patients. LAA was generated from 4D-CT data according to CT values with a threshold of less than -860 Hounsfield units (HU). Functional lung image was defined as the area where LAA was excluded from contralateral lung image. Two radiation therapy plans were designed: (1) Plan C, conventional VMAT and (2) Plan F, functional VMAT plan based on the functional lung. Both plans were compared in each patient with respect to the following dosimetric parameters: fV20, V20, fV10, V10, fV5, and V5, the percentages of functional or contralateral lung volumes irradiated with >20 Gy, 10 Gy, or 5 Gy, respectively; functional mean lung dose (fMLD) and mean lung dose (MLD), the mean dose to the functional or contralateral lung, respectively; maximum dose to the cord; mean doses to the liver and heart; and planning target volume homogeneity index.

**Results:** fV5 and MLD were significantly lower in Plan F (fV5, median 57.5% in Plan C vs 38.5% in Plan F,  $P < .01$ ; MLD, median 7.0 Gy in Plan C vs 6.4 Gy in Plan F,  $P = .04$ ). fV10, V5, and fMLD were also significantly lower in Plan F. Compared with Plan C, planning target volume homogeneity index and liver, heart, and cord doses were not significantly elevated in Plan F.

Conflicts of interest: None.

\* Corresponding author. Department of Radiation Oncology, Hiroshima University Hospital, 1-2-3, Kasumi, Minami-ku, Hiroshima City, 734-8551, Japan.

E-mail address: [tkkimura@hiroshima-u.ac.jp](mailto:tkkimura@hiroshima-u.ac.jp) (T. Kimura)

<http://dx.doi.org/10.1016/j.adro.2017.01.011>

2452-1094/© 2017 the Authors. Published by Elsevier Inc. on behalf of the American Society for Radiation Oncology. This is an open access article under the CC BY-NC-ND license (<http://creativecommons.org/licenses/by-nc-nd/4.0/>).

**Conclusions:** Significant reductions in fV5, fV10, fMLD, V5, and MLD were achieved with the functional image guided VMAT plan without negative effects on other factors. LAA-based functional image guided radiation therapy planning in VMAT is a feasible method to spare the functional lung in patients with MPM.

**Keywords:** Functional imaging, 4-dimensional computed tomography, image guided radiation therapy

© 2017 the Authors. Published by Elsevier Inc. on behalf of the American Society for Radiation Oncology. This is an open access article under the CC BY-NC-ND license (<http://creativecommons.org/licenses/by-nc-nd/4.0/>).

## Introduction

Malignant pleural mesothelioma (MPM) is a rare cancer that is most commonly caused by exposure to asbestos.<sup>1</sup> MPM is a life-threatening disease that is characterized by an extremely invasive local growth pattern.<sup>2</sup> However, MPM remains localized to a single hemithorax in its early stages, and therapeutic efforts have therefore focused on local treatment modalities.<sup>3,4</sup> Currently, trimodal therapy, consisting of chemotherapy, extrapleural pneumonectomy (EPP), and hemithorax radiation therapy, is recommended to improve local control.<sup>5–8</sup> Recently, intensity modulated radiation therapy (IMRT), including volumetric modulated arc therapy (VMAT), has been designed to allow for more effective conservation of normal tissue and better conformal high-dose irradiation for improved coverage of the contralateral thorax compared with 3-dimensional conformal radiation therapy.<sup>9–13</sup> Beginning in 2011, we initiated treatment planning with VMAT techniques after EPP for patients with MPM.<sup>14</sup>

A potential limitation of IMRT/VMAT in MPM is the necessity of low-dose radiation to the entire contralateral lung. A high rate of death due to radiation pneumonitis (RP) after IMRT was reported in the initial experience of the IMRT technique because a high radiation dose was administered to the entire contralateral lung.<sup>15</sup> Currently, the incidence of grade  $\geq 3$  RP after IMRT, evaluated according to the Common Terminology Criteria for Adverse Events, Version 4, has remained constant at 12% to 20%.<sup>11,14,16</sup> Therefore, there is a clinical need for safer methods of irradiation after EPP in patients with MPM.

Total and functional lung doses in patients with lung cancer were further reduced by the use of functional lung image-derived low attenuation areas (LAAs)<sup>17,18</sup> LAAs were based on 4-dimensional computed tomography (CT) scans and solely described nonfunctional lung regions. The incorporation of functional lung imaging, accounting for low alveolar density regions, has been associated with a risk of developing radiation pneumonitis in patients who are treated for lung cancer.<sup>18–21</sup> We believe this finding is also applicable to patients with MPM; therefore, we expect further reductions in total and functional doses to the lung.

The purpose of the present study was to evaluate the feasibility of sparing functional lung image-derived LAAs on the basis of 4-dimensional CT scans after EPP in patients with MPM.

## Methods and materials

### Patient background

A total of 12 male patients with MPM who had undergone definitive radiation therapy after extrapleural pneumonectomy (EPP) at Hiroshima University Hospital from 2010 to 2013 were enrolled in the present simulation study. All patients had a history of exposure to asbestos fibers; however, the results of pulmonary function tests after EPP were within the normal range. All patients underwent free-breathing CT and respiratory-gated 4-dimensional CT scans in the treatment position on the same day as treatment planning. We confirmed respiratory motions in the organs at risk (OAR) on 4-dimensional CT images and incorporated this information in the free-breathing CT image planning. Pathologic diagnoses, stages (Union for International Cancer Control, 7th edition), and primary tumor locations are summarized in [Table 1](#).

### Functional lung image-derived LAA based on 4-dimensional CT

Initially, 4-dimensional CT scans were acquired at a slice thickness of 2.5 mm on a multidetector row CT scanner (MDCT; LightSpeed, GE Medical Systems, Waukesha, WI) in cine mode with the Varian Real-Time Position Management Respiratory Gating system (Varian Medical Systems, Palo Alto, CA). After image acquisition, CT image data sets were sorted into 10-phase respiratory cycle bins, and a phase-by-phase evaluation was performed on a workstation (AdvantageSim; GE Healthcare, Princeton, NJ). The 10-phase set ranged from 0% to 90% in steps of 10%, with either 0% or 90% as the 0% end-inspiratory phase and 50% as the end-expiratory phase. All 10-phase CT data sets and free-breathing CT images were imported into the Eclipse treatment planning system (Varian Medical Systems).

**Table 1** Characteristics of study patients

Case Patient	Age (y)	Sex	Histology	TNM	Stage	Primary Location
1	68	M	Sarcomatous	pT1N0M0	IB	R
2	60	M	Epithelial	pT2N0M0	II	R
3	78	M	Epithelial	pT2N0M0	II	L
4	70	M	Epithelial	pT2N2M0	III	R
5	64	M	Biphasic	pT3N0M0	III	L
6	66	M	Epithelial	pT3N2M0	III	L
7	63	M	Epithelial	pT2N0M0	II	L
8	67	M	Biphasic	pT2N1M0	III	R
9	65	M	Biphasic	pT3N0M0	III	L
10	72	M	Epithelial	pT2N0M0	II	L
11	67	M	Epithelial	pT3N2M0	III	R
12	68	M	Epithelial	pT1N0M0	IB	R

L, left side, M, male; R, right side.

Several authors have reported threshold CT values for LAA detection and quantification that range from  $-850$  to  $-950$  Hounsfield units (HU).<sup>21–23</sup> We calculated LAA on the Eclipse from 10-phase, 4-dimensional CT data sets at a threshold of CT values lower than  $-860$  HU. Normal functional lung was defined as the area of total contralateral lung minus the LAA.<sup>17</sup> Figure 1 shows the 3 steps involved in calculating functional lung image-derived LAA on the basis of 4-dimensional CT scans in case 5: (1) acquisition of LAA at each phase (threshold =  $-860$  HU); (2) fusion of LAA at 3 expiratory phases (0%-90%) on a free-breathing CT image and trimming of the region of interest on the LAA image (0%-90%); and (3) definition of the functional lung image as the area where the LAA image (0%-90%) was subtracted from the free-breathing CT image. None of the steps in this technique used any type of deformable image registration algorithm.

## Target delineation

For the target delineation of each plan, the clinical target volume (CTV) included the entire preoperative ipsilateral hemithorax, scars, drain sites, and involved nodal stations. In general, the upper border of the CTV was 10 mm superior to the apex of the contralateral hemithorax and the lower border was the posterior diaphragmatic sulcus, which may reach as far posteriorly as the L2 vertebra, according to a study by Scherpereel et al.<sup>24</sup> This CTV definition also incorporated breathing movements that were determined with a 4-dimensional CT scan, positive surgical margins, and areas where there was a risk of dissemination, such as biopsy tracks in the chest wall, surgical scars, and sites of chest drains. The planning target volume (PTV) was delineated by a uniform 5-mm margin around the CTV. Normal tissue organs, including the total contralateral lung, liver, heart, esophagus, kidneys, spleen, and spinal cord, were delineated.

## Simulation methods of Plan C and Plan F

In this simulation study, 2 radiation therapy plans were designed and compared for each patient: Plan C was a conventional VMAT plan based on the total contralateral lung, and Plan F was a functional VMAT plan based on both the total contralateral and the functional lung. The details of OAR dose constraints in both plans are given in Table 2. We conducted the simulation study as follows: Plans were initially made with the most appropriate dose constraints for each patient (Plan C). The most appropriate priorities were defined individually on the basis of differences in patient characteristics, such as OAR volume. Plan F for each patient was designed in the same manner as Plan C for that patient. There were no changes in VMAT optimization objectives between Plan C and Plan F for each patient, with the exception of the consideration of functional lung regions. Supplementary Table 1 presents the details of the VMAT optimization for lungs in Plan C and Plan F.

A total dose of 54 Gy in 27 fractions delivered to 95% of the PTV was prescribed in both plans.<sup>1</sup> The prescribed dose was calculated using a heterogeneous dose calculation algorithm and a 2.5-mm grid (Eclipse anisotropic analytical algorithm; AAA, Version 11.0).

VMAT plans were generated on Eclipse treatment planning systems with 3 coplanar arcs (1 clockwise and 2 counter clockwise) with gantry rotation angles of  $220^\circ$  (ranging from  $40^\circ$ - $181^\circ$  and  $181^\circ$ - $40^\circ$  for right-sided primary tumors and from  $179^\circ$ - $320^\circ$  and  $320^\circ$ - $179^\circ$  for left-sided primary tumors) to avoid the entire contralateral lung. The collimator angle of each arc was set to  $10^\circ$  or  $80^\circ$  to avoid a tongue-and-groove effect. Treatment plans were delivered using 10-MV photons that were generated by a linear accelerator (CLINAC iX; Varian Medical Systems) with continuous changes in gantry speed, multi-leaf collimator position, and dose rate. The equipped millennium multi-leaf collimators comprised 120 leaves (leaf widths at the isocenter were 5 mm in the central 20-cm region of the field and 10 mm in the outer  $2 \times 10$  cm regions, with a leaf transmission of 1.7%). The same beam arrangements were used for both plans.

## Data analysis and statistical methods

We evaluated the dosimetric parameters of Plans C and F: (1) lung V5-20 and fV5-20, the percentage of total and functional lung irradiated volumes with 5 Gy to 20 Gy, respectively; (2) mean lung dose (MLD) and functional MLD (fMLD), the mean doses that were delivered to the total contralateral lung and functional lung, respectively; (3) D98 (Gy) and D50 (Gy) of PTV (ie, the dose receiving  $\geq 98\%$  and  $\geq 50\%$  of PTV volume, respectively), V95% (%) of PTV (ie, the volume receiving  $\geq 95\%$  of prescribed dose/PTV volume), mean dose, and homogeneity index

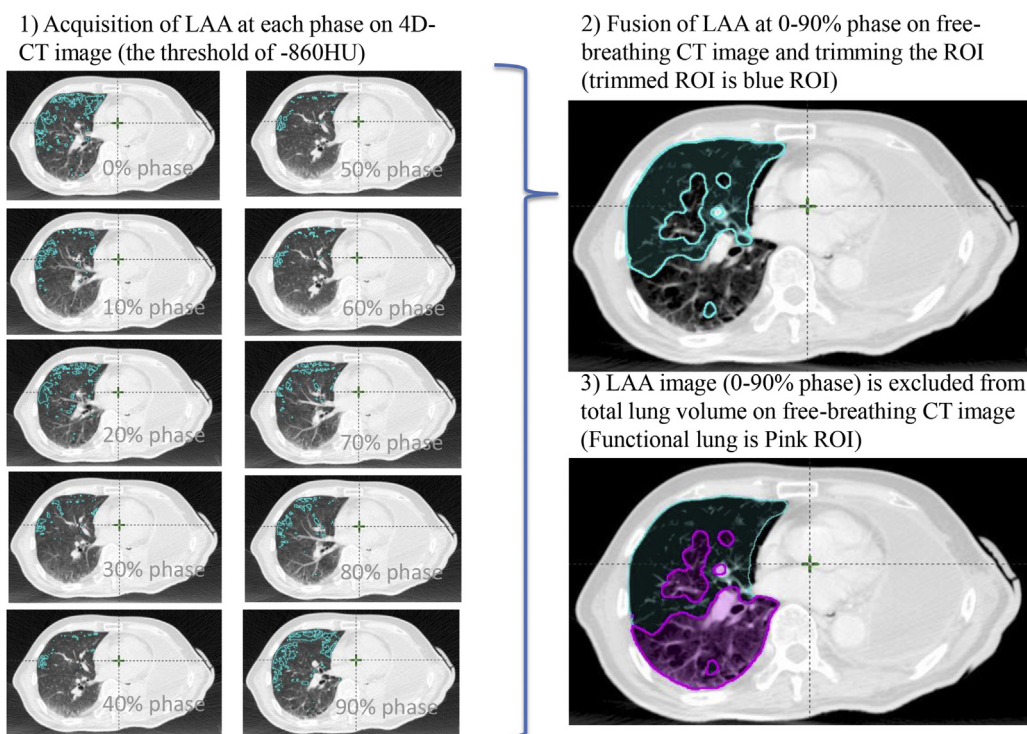


**Figure 1** Calculation of functional lung volume. First, low attenuation areas (LAA) are automatically delineated in all phases of 4-dimensional computed tomography (CT) images (blue area). Next, all phases of LAA are fused on free-breathing planning CT images and trimmed. Finally, trimmed LAA images are excluded from the total lung on free-breathing planning CT images, and residual areas are designated as the functional lung (pink area).

(HI) of PTV (where  $HI = \text{maximum dose of PTV}/54 \text{ Gy}$ ); and (4) mean and V20 and V30 of liver (ie, the percentage of liver irradiated volumes with 20 Gy and 30 Gy, respectively), V40 and V50 of heart (ie, the percentage of heart irradiated volumes with 20 Gy and 30 Gy, respectively), and maximum dose of spinal cord.

When comparing normal tissues other than those from the lung, we independently evaluated the right and

left side of primary locations because irradiation doses to the liver and heart differ depending on the primary location. Box-and-whisker plotting and Wilcoxon signed-rank test were used for all comparisons between treatment plans, and  $P < .05$  was considered statistically significant.

## Results

### Details of clinical characteristics

The average total contralateral lung volume in both plans was  $1824.3 \pm 268.6 \text{ mL}$  ( $1580.6\text{--}2231.2 \text{ mL}$ ). The average functional lung volume was  $888.4 \pm 353.7 \text{ mL}$  ( $273.2 \text{ ml}\text{--}1573.7 \text{ mL}$ ). The mean proportion of the total contralateral lung covered by the calculated LAA was 46.6%.

### Comparison of dosimetric parameters of the contralateral lung

The values of the dosimetric parameters fV5, fV10, fMLD, V5, and MLD were significantly lower for Plan F compared with those for Plan C (fV5, median 57.5% for Plan C vs 38.5% for Plan F,  $P < .01$ ; fV10, median 14.8% for Plan C vs 8.9% for Plan F,  $P < .01$ ; fMLD,

**Table 2** Dose constrains for organs at risk

Organs at Risk	Index	Plan C	Plan F
Contralateral Lung	Mean dose	<8 Gy	<8 Gy
	V5 <sup>a</sup>	<60%	<60%
	V10 <sup>a</sup>	<20%	<20%
	V20 <sup>a</sup>	<10%	<10%
Functional lung	V5 <sup>a</sup>	-	<40%
	V10 <sup>a</sup>	-	<10%
	V20 <sup>a</sup>	-	<5%
Liver	Mean dose	<30 Gy	<30 Gy
	V30 <sup>b</sup>	<30%	<30%
Heart	Maximal dose	<60 Gy	<60 Gy
	V45 <sup>c</sup>	<30%	<30%
Spinal cord	Maximal dose	<50 Gy	<50 Gy

<sup>a</sup> V5, V10, and V20 are the percentages of the contralateral lung and functional lung volume that receive  $\geq 5$ ,  $\geq 10$ , and  $\geq 20$  Gy, respectively.

<sup>b</sup> V30 is the percentage of the liver volume that receives  $\geq 30$  Gy.

<sup>c</sup> V45 is the percentage of the heart volume that receives  $\geq 45$  Gy.

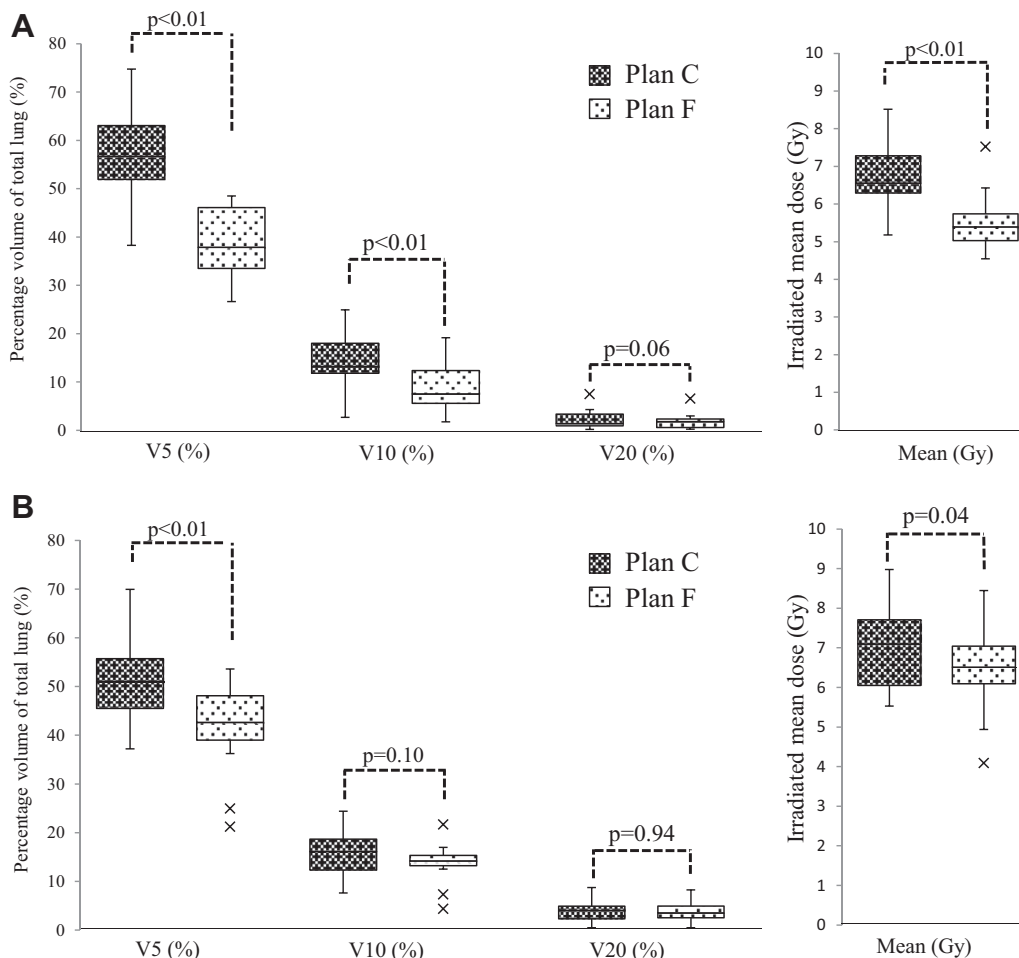


**Figure 2** Box-and-whisker plots show the percentage volume of (A) functional and (B) total contralateral lungs receiving the V5, V10, V20, and irradiated mean dose. The band inside the box represents the median and the bottom and top of the box represent the 25<sup>th</sup> and 75<sup>th</sup> percentiles. The whiskers indicate the lowest datum still within the 1.5 interquartile range (IQR) of the lower quartile and the highest datum still within the 1.5 IQR of the upper quartile. Crosses (“x”) indicate outliers of maximum displacement. Plan F significantly reduced V5 (38.5%), V10 (8.9%), and MLD (5.5 Gy) in the functional lung and V5 (41.6%) and MLD (6.4 Gy) in the contralateral lung compared with Plan C.

median 6.8 Gy for Plan C vs 5.5 Gy for Plan F,  $P < .01$ ; V5, median 51.4% for Plan C vs 41.6% for Plan F,  $P < .01$ ; MLD, median 7.0 Gy for Plan C vs 6.4 Gy for Plan F,  $P = .04$ ). No significant differences in fV20, V10, or V20 were observed across the plans. However, fV20, V10, and V20 were lower for Plan F compared with those for Plan C. **Figure 2** compares the results for functional contralateral lungs (A) and total contralateral lungs (B). **Figure 3** shows the dose distribution in Case 7.

**Comparison of dosimetric parameters for PTV and OAR**

No significant differences in PTV D98% dose, mean dose, D50% dose, V95%, HI, or irradiation doses to the liver, heart, and spinal cord were observed between Plan C and Plan F. **Figure 4** shows the dosimetric parameters

of (A) PTV and (B) liver, (C) heart, and (D) spinal cord between Plan C and Plan F.

**Discussion**

The present study demonstrated LAA-based planning of functional image guided radiation therapy could improve pulmonary dosimetric parameters without requiring a major change in PTV coverage or increasing irradiation doses to other OAR. According to several previous studies, IMRT was designed to provide conformal high-dose irradiation for improved coverage of the hemithorax, which has a complex shape, in patients with MPM after EPP.<sup>9–12</sup> However, patients with MPM only have the contralateral lung after EPP; therefore, the number of deaths caused by radiation pneumonitis has reportedly increased due to the high volume of low

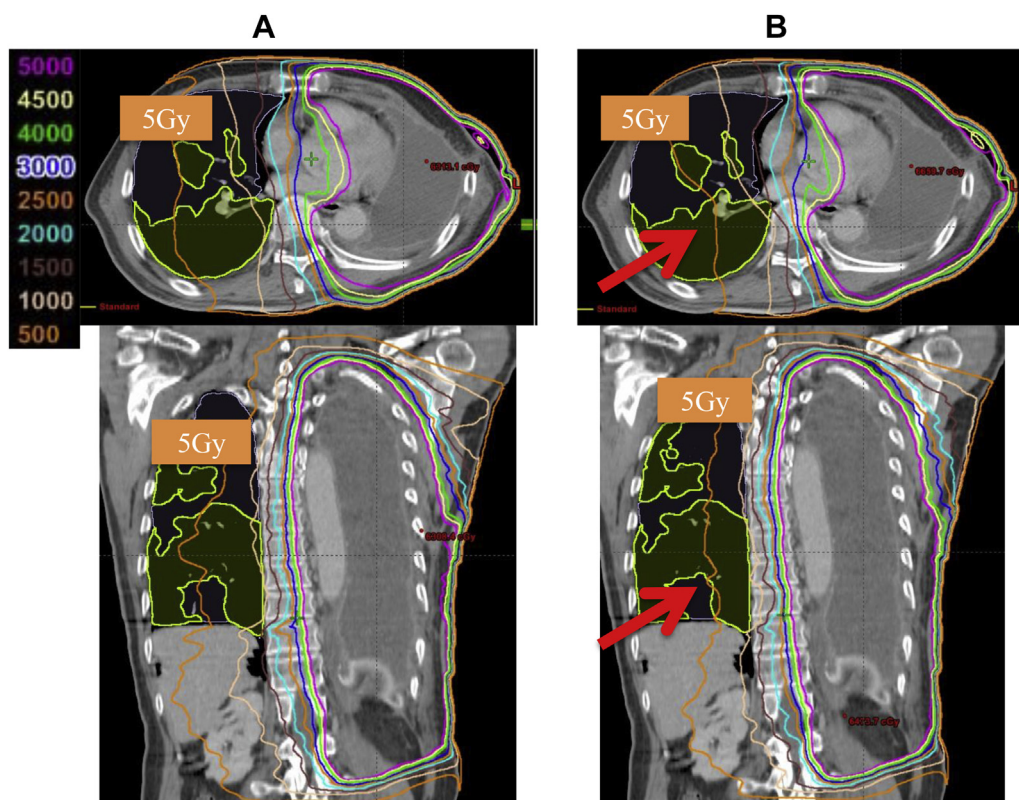


**Figure 3** Comparison of dose distribution between (A) Plan C and (B) Plan F in Case 7. The  $\geq 5$  Gy isodose line is shown in orange and the functional lung area in green. The  $\geq 5$  Gy isodose line was reduced in the functional lung for Plan F (red arrows).

irradiation areas, such as V5, administered to the entire contralateral lung.<sup>15</sup>

We believe that there is a significant clinical need to reduce pulmonary irradiation doses as much as possible. In addition, the lungs of patients with MPM differ considerably from healthy normal lungs due to these patients' history of exposure to asbestos, thereby making it important that irradiated contralateral lung volumes are reduced. Asbestos fibers are never removed from the body once absorbed and thus cause chronic inflammation. After repeated damage to peripheral lung regions, pulmonary fibrosis and emphysematous-associated changes gradually appear in exposed individuals<sup>25,26</sup> These changes result in a severely impaired gas exchange and may lead to the development of combined pulmonary fibrosis and emphysema (CPFE) syndrome.<sup>27,28</sup>

A previous study reported that 40% of patients with CPFE have a history of exposure to asbestos with a strong correlation described between MPM and risk of developing CPFE.<sup>28,29</sup> These conditions rarely improve and negatively affect both morbidity and mortality in individuals who were exposed to asbestos even after decades of nonexposure.<sup>26</sup> Lungs that have been exposed to asbestos fibers may be more easily damaged and more susceptible to pulmonary function degradation when compared with healthy lungs. Pulmonary function preservation should be considered from the start of trimodal

treatment, even in patients who are asymptomatic at the time of diagnosis.

Several authors have investigated functional imaging modalities, such as ventilation imaging based on 4-dimensional CT scans and perfusion imaging based on single-photon emission computed tomography, to reduce radiation lung doses.<sup>18–20,30,31</sup> Yamamoto et al. demonstrated a correlation between pulmonary function and low-density CT regions using 4-dimensional CT images with deformable image registration in a cohort of patients with thoracic cancer.<sup>20</sup>

We also demonstrated that lung dose and 4-dimensional CT ventilation-based function were correlated with thoracic clinical toxicity after radiation therapy.<sup>18</sup> The LAA technique used in the present study can be performed more easily than those described in other reports because LAA does not require a sophisticated deformable image registration algorithm. Currently, no studies have demonstrated evidence of a correlation between lower irradiation lung areas, such as V5, and the clinical outcomes of MPM after EPP. However, the incidence of fatal pulmonary toxicity seemed to occur in patients who received relatively higher doses to the contralateral lung.

At Brigham and Women's Hospital, of 13 patients who received EPP followed by IMRT, 6 (46%) died of RP. The median V5 for the patients who developed pneumonitis

Plan C  
Plan F

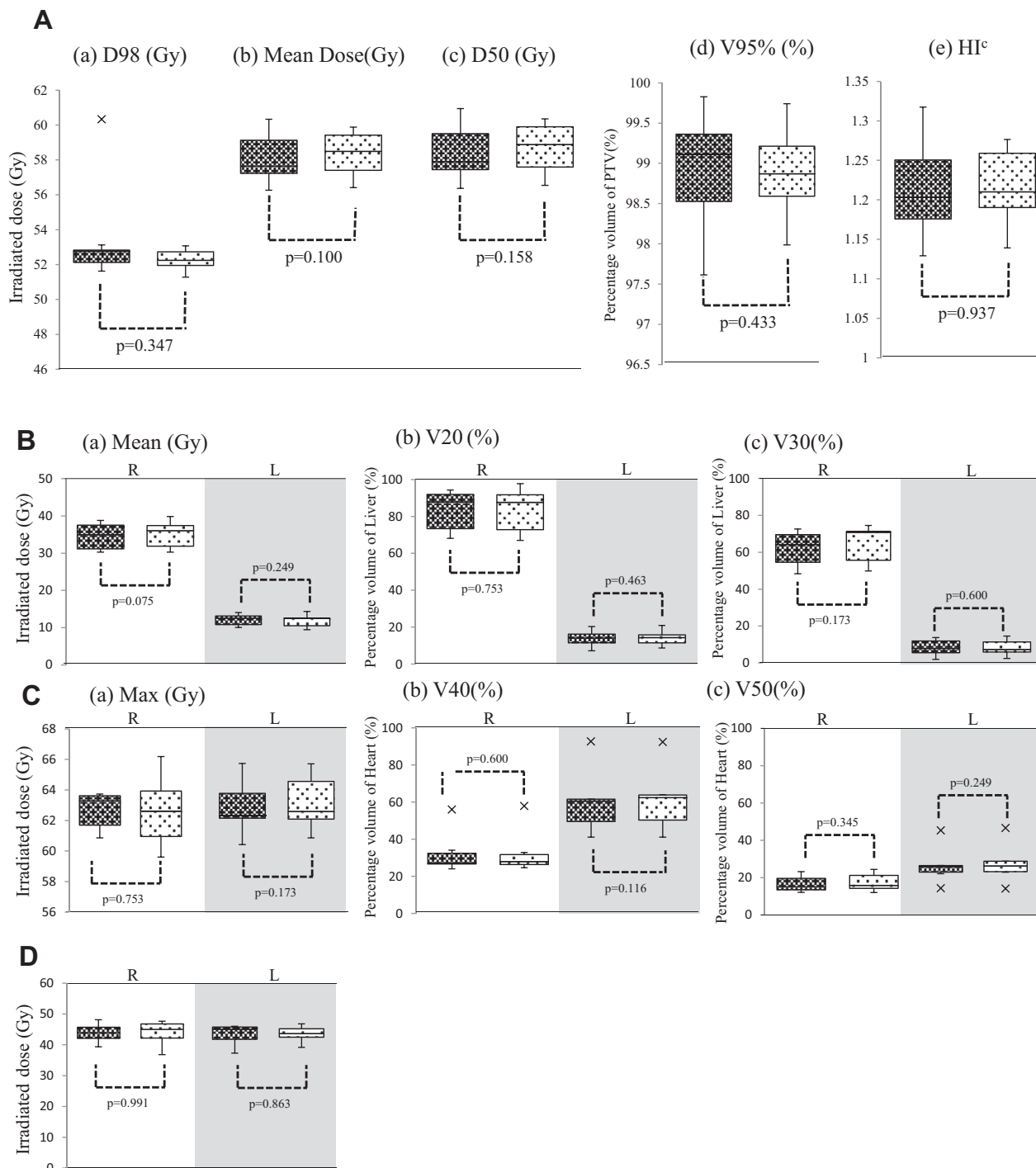


**Figure 4** Box-and-whisker plots show (A) D98 (Gy), D50 (Gy), irradiated mean dose, V95 (%), and homogeneity index to the planning target volume; (B) V20 (%), V30 (%), and irradiated mean dose to the liver; (C) V40 (%), V50 (%), and irradiated mean dose to the heart; and (D) maximum irradiated dose to the spinal cord. There are no significant differences in organs at risk between Plan C and Plan F.

was 98.6% (range, 81.4%-100%).<sup>15</sup> Rice et al. reported that patients with a high V20 or MLD were at a greatly increased risk of fatal pulmonary toxicity.<sup>32</sup> Kristensen

et al. reported significant differences in MLD and V10 for patients with fatal pulmonary toxicity compared with patients without fatal lung toxicity.<sup>33</sup> Thus, V20, V10, V5,

and MLD evidently should be kept as low as possible to prevent fatal pulmonary toxicity.

To decrease the incidence of severe pulmonary toxicity, Chi et al. recommended limiting the MLD to <8.5 Gy, V5 to <60%, and V20 to <20% in the contralateral lung.<sup>34</sup> In this study, even with Plan C, MLD, V5, and V20 were very low (MLD, 7.0 Gy; V5, 51.4%; and V20, 4.0% in Plan C). Furthermore, we can achieve a lower MLD and V5 with Plan F than with Plan C (MLD, 6.4 Gy; V5, 41.6%; and V20, 4.0% in Plan F). Moreover, our plan would entail a reduced risk of RP for patients with MPM after EPP.

The present study has several limitations. We conjecture that there was no significant clinical impact because the number of patients with MPM was not sufficient at this stage. Furthermore, the proper CT value thresholds for LAA detection and quantification of the pulmonary function correlations determined using this method have yet to be validated in patients with MPM after EPP. Plan F had a greater tendency toward higher irradiation doses to OAR than Plan C. However, we believe these differences are within the clinically acceptable range because they did not reach statistical significance. In the future, prospective clinical trials will be required to determine the efficacy of this type of functional avoidance treatment planning to improve treatment outcomes such as survival and complication rates.

## Conclusions

Functional LAA-based image guided radiation therapy planning in VMAT appears to be effective in preserving functional lung volume in patients with MPM. Further investigations and prospective clinical trials are required to address the aforementioned technical issues related to LAA-based image guided planning.

## Supplementary data

Supplementary material for this article (<http://dx.doi.org/10.1016/j.adro.2017.01.011>) can be found at [www.practicalradonc.org](http://www.practicalradonc.org).

## References

- Murayama T, Takahashi K, Natori Y, Kurumatani N. Estimation of future mortality from pleural malignant mesothelioma in Japan based on an age-cohort model. *Am J Ind Med*. 2006;49:1-7.
- Sugarbaker DJ, Strauss GM, Lynch TJ, et al. Node status has prognostic significance in the multimodality therapy of diffuse, malignant mesothelioma. *J Clin Oncol*. 1993;11:1172-1178.
- Rusch VW, Rosenzweig K, Venkatraman E, et al. A phase II trial of surgical resection and adjuvant high dose hemithoracic radiation for malignant pleural mesothelioma. *J Thorac Cardiovasc Surg*. 2001;122:788-795.
- Pass HI, Kranda K, Temeck BK, Feuerstein I, Steinberg SM. Surgically debulked malignant pleural mesothelioma: results and prognostic factors. *Ann Surg Oncol*. 1997;4:215-222.
- Batirel HF, Metintas M, Caglar HB, et al. Trimodality treatment of malignant pleural mesothelioma. *J Thorac Oncol*. 2008;3:499-504.
- Weder W, Stahel RA, Bernhard J, et al. Multicenter trial of neo-adjuvant chemotherapy followed by extrapleural pneumonectomy in malignant pleural mesothelioma. *Ann Oncol*. 2007;18:1196-1202.
- Flores RM, Krug LM, Rosenzweig KE, et al. Induction chemotherapy, extrapleural pneumonectomy, and postoperative high-dose radiotherapy for locally advanced malignant pleural mesothelioma: A phase II trial. *J Thorac Oncol*. 2006;1:289-295.
- Yajnik S, Rosenzweig KE, Mychalczak B, et al. Hemithoracic radiation after extrapleural pneumonectomy for malignant pleural mesothelioma. *Int J Radiat Oncol Biol Phys*. 2003;56:1319-1326.
- Krayenbuehl J, Oertel S, Davis JB, Ciernik IF. Combined photon and electron three-dimensional conformal versus intensity-modulated radiotherapy with integrated boost for adjuvant treatment of malignant mesothelioma after pleuropneumonectomy. *Int J Radiat Oncol Biol Phys*. 2007;69:1593-1599.
- Scorsetti M, Bignardi M, Clivio A, et al. Volumetric modulation arc radiotherapy compared with static gantry intensity-modulated radiotherapy for malignant pleural mesothelioma tumor: A feasibility study. *Int J Radiat Oncol Biol Phys*. 2010;77:942-949.
- Giraud P, Sylvestre A, Zefkili S, et al. Helical tomotherapy for resected malignant pleural mesothelioma: Dosimetric evaluation and toxicity. *Radiother Oncol*. 2011;101:303-306.
- Patel PR, Yoo S, Broadwater G, et al. Effect of increasing experience on dosimetric and clinical outcomes in the management of malignant pleural mesothelioma with intensity-modulated radiation therapy. *Int J Radiat Oncol Biol Phys*. 2012;83:362-368.
- Kimura T, Doi Y, Nakashima T, et al. Clinical experience of volumetric modulated arc therapy for malignant pleural mesothelioma after extrapleural pneumonectomy. *J Radiat Res*. 2015;56:315-324.
- Allen AM, Czerminska M, Jänne PA, et al. Fatal pneumonitis associated with intensity-modulated radiation therapy for mesothelioma. *Int J Radiat Oncol Biol Phys*. 2006;65:640-645.
- Gomez DR, Hong DS, Allen PK, et al. Patterns of failure, toxicity, and survival after extrapleural pneumonectomy and hemithoracic intensity-modulated radiation therapy for malignant pleural mesothelioma. *J Thorac Oncol*. 2013;8:238-245.
- Kimura T, Nishibuchi I, Murakami Y, et al. Functional image-guided radiotherapy planning in respiratory-gated intensity-modulated radiotherapy for lung cancer patients with chronic obstructive pulmonary disease. *Int J Radiat Oncol Biol Phys*. 2012;82:e663-e670.
- Krayenbuehl J, Riesterer O, Graydon S, Dimmerling P, Kloeck S, Ciernik IF. Intensity-modulated radiotherapy and volumetric-modulated arc therapy for malignant pleural mesothelioma after extrapleural pleuropneumonectomy. *J Appl Clin Med Phys*. 2013;14:1-10.
- Marks L, Spencer DP, Sherouse GW, et al. The Role of three dimensional functional lung imaging in radiation treatment planning: the functional dose-volume histogram. *Int J Radiat Oncol Biol Phys*. 1995;33:65-75.
- Yamamoto T, Kabus S, Lprenz C, et al. Pulmonary ventilation imaging based on 4-dimensional computed tomography: comparison with pulmonary function tests and SPECT ventilation images. *Int J Radiat Oncol Biol Phys*. 2014;90:414-422.
- Kimura T, Doi Y, Nakashima T, et al. Combined ventilation and perfusion imaging correlate with the dosimetric parameters of radiation pneumonitis in radiotherapy planning for lung cancer. *Int J Radiat Oncol Biol Phys*. 2015;93:778-787.
- Park KJ, Bergin CJ, Clausen JL. Quantitation of emphysema with three-dimensional CT densitometry: Comparison with two-dimensional

- analysis, visual emphysema scores, and pulmonary function test results. *Radiology*. 1999;211:541-547.
22. Gevenois PA, Vuyst PD, Sy M, et al. Pulmonary emphysema: Quantitative CT during expiration. *Radiology*. 1996;199:825-829.
  23. Matsuoka S, Kurihara Y, Yagihashi K, Hoshino M, Watanabe N, Nakajima Y. Quantitative assessment of air trapping in chronic obstructive pulmonary disease using inspiratory and expiratory volumetric MDCT. *AJR Am J Roentgenol*. 2008;190:762-769.
  24. Scherpereel A, Astoul P, Baas P, et al. Guidelines of the European Respiratory Society and the European Society of Thoracic Surgeons for the management of malignant pleural mesothelioma. *Eur Respir J*. 2010;35:479-495.
  25. Vehmas T, Oksa P, Kivisaari L. Lung and pleural CT signs predict deaths: 10-year follow-up after lung cancer screening of asbestos-exposed workers. *Int Arch Occup Environ Health*. 2012;85:207-213.
  26. Huuskonen O, Kivisaari L, Zitting A, Keleva S, Vehmas T. Emphysema finding associated with heavy asbestos-exposure in high resolution computed tomography of Finnish construction workers. *J Occup Health*. 2004;46:266-271.
  27. Ando K, Sekiya M, Tobino K, Takahashi K. Relationship between quantitative CT metrics and pulmonary function in combined pulmonary fibrosis and emphysema. *Lung*. 2013;191:585-591.
  28. Cottin V, Nunes H, Brillet PY, et al. Combined pulmonary fibrosis and emphysema: A distinct underrecognised entity. *Eur Respir J*. 2005;26:586-593.
  29. Mitsuoka S, Yamashiro T, Matsushita S, et al. Quantitative CT evaluation in patients with combined pulmonary fibrosis and emphysema. *Acad Radiol*. 2015;22:626-631.
  30. Yamamoto T, Kabus S, Berg JV, Lorenz C, Keall PJ. Impact of four-dimensional computed tomography pulmonary ventilation imaging-based functional avoidance for lung cancer radiotherapy. *Int J Radiat Oncol Biol Phys*. 2011;79:279-288.
  31. Shioyama Y, Jang SY, Liu HH, et al. Preserving functional lung using perfusion imaging and intensity-modulated radiation therapy for advanced-stage non-small cell lung cancer. *Int J Radiat Oncol Biol Phys*. 2006;68:562-571.
  32. Rice DC, Stevens CW, Correa AM, et al. Outcomes after extrapleural pneumonectomy and intensity-modulated radiation therapy for malignant pleural mesothelioma. *Ann Thorac Surg*. 2007;84:1685-1692.
  33. Kristensen CA, Notttrup TJ, Berthelsen AK, et al. Pulmonary toxicity following IMRT after extrapleural pneumonectomy for malignant pleural mesothelioma. *Radiother Oncol*. 2009;92:96-99.
  34. Chi A, Liao Z, Nguyen NP, et al. Intensity-modulated radiotherapy after extrapleural pneumonectomy in the combined modality treatment of malignant pleural mesothelioma. *J Thorac Oncol*. 2011;6:1132-1141.